

Atlas-based approach to study white matter disruption in Alzheimer's disease

X. Fan¹, G. Xiao², K. Martin-Cook³, R. Rosenberg³, M. Weiner⁴, and H. Huang¹

¹Advanced Imaging Research Center, University of Texas Southwestern Medical Center, Dallas, TX, United States, ²Department of Clinical Sciences, University of Texas Southwestern Medical Center, Dallas, TX, United States, ³Department of Neurology, University of Texas Southwestern Medical Center, Dallas, TX, United States, ⁴Department of Psychiatry, University of Texas Southwestern Medical Center, Dallas, TX, United States

Introduction

DTI-derived metrics, fractional anisotropy (FA), has been widely used to detect subtle structural white matter abnormalities. Conventional VBM (voxel-based-morphometry) approaches delineate the abnormality at the voxel level. However, information reflected from a single voxel of the brain image cannot be used to evaluate the clinical condition of the patient. It is the whole white matter tracts connecting different brain regions that have clinical importance. In this study, the targeted unit is the functional white matter tract incorporating continuous and multiple voxels rather than the individual voxel in a brain image. We developed a method to survey all white matter tracts by mapping the labeling of a digital atlas [1] to the core white matter [2] of the subjects and applied it to Alzheimer disease (AD). With no *a priori* information, this novel atlas-based approach has been used to examine all 50 major white matter tracts of AD patients and age-matched controls at the tract level. The proposed method is highly efficient, accurate, makes comprehensive examination of all major tracts and allows comparison of disruption level of these tracts. With the analysis of AD results, we found that white matter disruption in AD brains is heterogeneous, widespread, and affects the fornix most severely.

Methods

Subjects and data acquisition: A total of 38 subjects (20 AD and 18 age-matched normal subjects) were recruited for this study from longitudinally followed cohorts of the Alzheimer's Disease Neuroimaging Initiative (ADNI). A 3T Philips Achieva MR system was used. DTI data were acquired using a single-shot EPI with SENSE. DWI parameters were: FOV=224/224/143mm, in plane imaging matrix = 112× 112, axial slice thickness = 2.2 mm, 30 independent diffusion-weighted directions with b-value = 1000 sec/mm², TE=97ms, TR=7.6s. To increase signal noise ratio (SNR), two repetitions were performed. **Atlas-based quantification at the tract level:** FA data of all subjects were first nonlinearly registered to the so-called "EVE" template, which is FA data of an individual subject serving as the template to set up ICBM-DTI-81 atlas [1]. This step ensures that all our FA data is well registered to the ICBM-DTI-81 atlas. As shown in Fig 1a, tract-based spatial statistics (TBSS) [2] of FSL was used to project the FA value of white matter to the skeleton or core of the white matter with FA data of all subjects at the template space. Fig. 1b is the ICBM-DTI-81 atlas. By transferring the labeling of the individual white matter tract, for example, genu of corpus callosum (GCC), we can label the skeleton FA data of all subjects in the template space, as shown in Fig. 1c. In this way, the atlas data were overlaid to the mean skeleton in the ICBM-DTI-81 space such that each skeleton voxel could be categorized into one of the 50 major tracts. **Statistical analysis to compare FA at tract level:** For a more accurate analysis, we have taken the FA values of all voxels projected to the skeleton within each white matter tract, rather than averaged FA of a tract, as the data source to detect FA reduction in AD group compared to age-matched controls. As FA measurements for the voxels within the same tract were highly correlated, the mixed-effects model was fitted for each tract to account for these correlations. The spatial correlation among voxels was explored using variogram and goodness of fit was checked by residual plots and Akaike Information Criterion. The false discovery rate (FDR) was used to control the family-wise type-I error.

Results

Parcellation of white matter tracts with the digital atlas: The JHU ICBM-DTI-81 atlas assigns a unique label, one of integer values from 0 to 50, to each voxel in the ICBM-DTI-81 space to indicate that the voxel belongs to one of 50 well-documented deep white matter tracts. Shown in Fig. 2, the atlas data were overlaid on the mean skeleton in the ICBM-DTI-81 space such that each skeleton voxel is categorized into one of the 50 major tracts. As the template for nonlinear registration in TBSS and that used for generating the ICBM-DTI-81 are the same, labeled white matter regions from the atlas match the mean FA map well and cover the entire tract skeleton, demonstrating the effectiveness and accuracy of this novel atlas-based analysis process. **FA difference:** White matter tracts which had significantly lower FA values with p (FDR-corrected) <0.05 in the AD group are listed in Table 1. It lists complete statistics for FA differences in terms of the mean FA difference, t values and FDR-corrected p values. The white matter tracts are summarized in the order of FDR-corrected p values. It shows that the white matter disruption is widespread. The disrupted tracts include limbic, callosal, projection and association tracts; the fornix is the most severely affected in AD subjects.

Conclusion and discussion

We developed a novel white matter atlas-based analysis method to survey all white matter at the tract level and applied it to a group of AD subjects and controls. This approach integrates the core white matter projection function in TBSS, digital white matter atlas JHU ICBM-DTI-81 and mixed-effects statistical model to perform the group analysis with all FA values of a segmented white matter tract. It can perform a complete assessment of all white matter. By ranking the t value, we found that the fornix is most severely affected. Integrity changes of all the tracts in Table 1 have been reported in the literatures, demonstrating the accuracy and efficiency of our method. Compared to conventional VBM approach, the group analysis is at the tract level, which may provide invaluable information in following and predicting the course of AD. The whole process is automated and has the potential to be used in detecting abnormality of white matter at the tract level in other disease models.

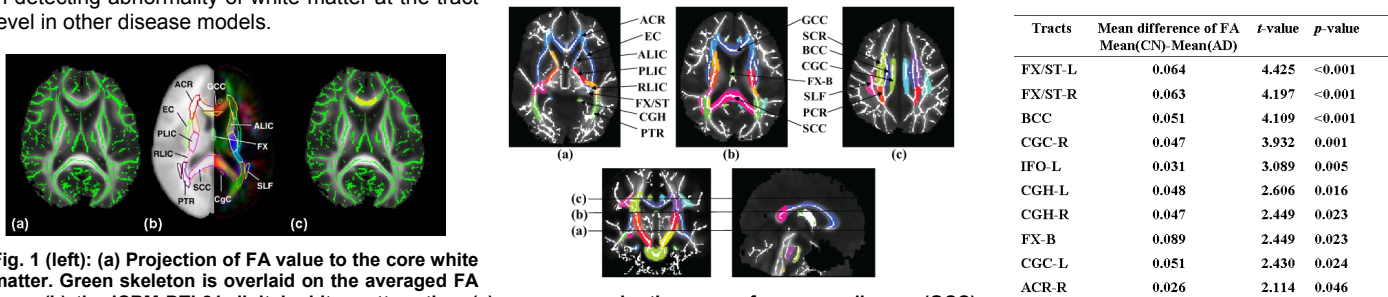


Fig. 1 (left): (a) Projection of FA value to the core white matter. Green skeleton is overlaid on the averaged FA map; (b) the ICBM-DTI-81 digital white matter atlas; (c) as an example, the genu of corpus callosum (GCC) (yellow shadow) is transferred from the digital atlas to cover the green skeleton overlaid on the averaged FA map. Abbreviations of the white matter tract names can be found in the legend of Fig. 2.

Fig. 2 (middle): Mean FA (gray scale) and skeleton of all subjects overlaid by the atlas labels. Colored region indicate major white matter tracts. The skeleton from averaged FA maps is shown as white solid curve. Abbreviations of white matter tracts are as follows. ACR: Anterior corona radiata; ALIC: Anterior limb of internal capsule; BCC: Body of corpus callosum; CGC: Cingulum; CGH: Cingulum (hippocampus); CST: Corticospinal tract; EC: External capsule; FX: Fornix FX-B: Body of fornix; GCC: Genu of corpus callosum; IFO: Inferior fronto-occipital fasciculus left; PCR: Posterior corona radiate; PLIC: Posterior limb of internal capsule; PTR: Posterior thalamic radiation; RLIC: Retrolenticular part of internal capsule; SCC: Splenium of corpus callosum; SCR: Superior corona radiate; SLF: Superior longitudinal fasciculus; ST: Stria terminalis; UNC: Uncinate fasciculus.

Table 1 (right): List of group statistics on FA for disrupted white matter tracts of AD patients, ordered with p values. p values are after FDR correction. Only the tracts with FDR corrected p<0.05 are listed.

References: [1] Mori, S et al (2008) NeuroImage 40: 572. [2] Smith, SM et al (2006) NeuroImage 31:1487. **Acknowledgement:** This study is sponsored by NIH/NIA P30AG12300, NIH RR014982 and NIH EB009545.